RSC Mechanochemistry

ROYAL SOCIETY OF CHEMISTRY

PAPER

View Article Online
View Journal

Cite this: DOI: 10.1039/d4mr00126e

Selective mechanochemical conversion of post-consumer polyethylene terephthalate waste into hcp and fcu UiO-66 metal–organic frameworks†

Tomislav Stolar, *[a] Dilara Bayram,[ab] Anastasia May,[a] Remie Sundermann,[ac] Carsten Prinz,[a] Klas Meyer,[a] Anett Myxa,[a] Jana Falkenhagen[a] and Franziska Emmerling *[a]

Received 28th October 2024
Accepted 3rd January 2026

DOI: 10.1039/d4mr00126e

rsc.li/RSCMechanochem

Single-use plastics strongly contribute to plastic pollution, and less than 10% of plastic waste is recycled globally. Here, we present a selective mechanochemical protocol for converting post-consumer polyethylene terephthalate (PET) transparent bottles and coloured textile waste into the porous metal–organic framework (MOF) UiO-66 materials. We used time-resolved *in situ* (TRIS) synchrotron powder X-ray diffraction and Raman spectroscopy to monitor the depolymerization of PET during ball milling. To convert disodium terephthalate to UiO-66, we developed base and base-free synthetic routes that lead to fcu and hcp UiO-66 phases, respectively, including the first ever synthesis of hcp UiO-66 by mechanochemistry. Our results demonstrate the potential of mechanochemistry to selectively access fcu and hcp UiO-66 phases using post-consumer PET waste.

Introduction

Plastic materials are ubiquitous in many aspects of our lives and are produced on a massive scale globally (400 million tons in 2020).[1] However, we are facing a 'plastic crisis' due to single-use plastics, with only 10% of plastic waste recycled by 2021.[2] Most plastic waste is either landfilled or incinerated in an unsustainable manner. Plastic waste in the environment, including microplastics, poses a risk to ecosystems and humans,[2] and implementing recycling technologies is needed to establish a circular economy for plastics. The current state of the art is mechanical recycling, which produces lower quality and lower value products and cannot process all types of plastic waste streams.[3] From the perspective of sustainability and circularity, chemical recycling to monomers is an ideal approach as it is generally independent of a particular waste stream.[1] However, due to thermodynamic constraints, not all plastic polymers are amenable to chemical recycling into monomers and known technologies are often not cost-efficient and therefore not practical.[3] Chemical recycling technologies include pyrolysis, dissolution, and depolymerization. Pyrolysis is used for energy recovery from plastics but uses high temperatures and pressures, emits toxic gases, and in total results in an economic loss.[3] Dissolution uses toxic solvents, which in turn generate significant amounts of solvent waste that must be disposed of or recycled, raising sustainability concerns.[3]

Faced with these challenges, researchers have turned to innovative and sustainable approaches. Mechanochemistry has emerged as a promising approach for addressing United Nations Sustainable Development Goals,[4] including depolymerization of plastics.[5–8] In mechanochemistry,[9–11] mechanical action chemically breaks down plastic polymers without bulk solvents, in compliance with the principles of green chemistry and sustainability.[12,13] Recently, mechanochemical depolymerization of polystyrene,[14–17] poly(α-methyl styrene),[18] poly(methyl methacrylate),[19] polyethylene,[20–24] polypropylene,[25–27] polylactic acid,[28,29] furanoate-based polymers,[30] poly(vinyl chloride),[31] and PET[32–41] have been reported.

In the case of PET, Štrukil showed that post-consumer coloured PET bottles and PET textile waste can be used as starting materials for the mechanochemical depolymerization with sodium hydroxide (NaOH).[32] The use of milling equipment made of stainless steel (10 mL jar volume) and larger milling balls (one 15 mm stainless steel ball) was found to be helpful, indicating that higher mechanical loading was necessary to overcome the activation barrier for the ester bond hydrolysis. Interestingly, a change in rheology from a powder to a gum-like mixture was observed and correlated with the quantitative conversion to Na_2TP after 2 h of milling at 30 Hz. Shortly after the Štrukil report, Tricker *et al.* demonstrated that quantitative PET depolymerization to disodium terephthalate (Na_2TP) could

[a]Federal Institute for Materials Research and Testing (BAM), Richard-Willstätter-Str. 11, 12489 Berlin, Germany. E-mail: tomislav.stolar@bam.de; franziska.emmerling@bam.de

[b]Department of Pharmaceutical and Chemical Engineering, Berliner Hochschule für Technik, Berlin 13353, Germany

[c]IMT Mines Albi, CT Cedex 09, 81013 Albi, France

† This work is dedicated to Prof. Frédéric Lamaty on the occasion of his 60th birthday.

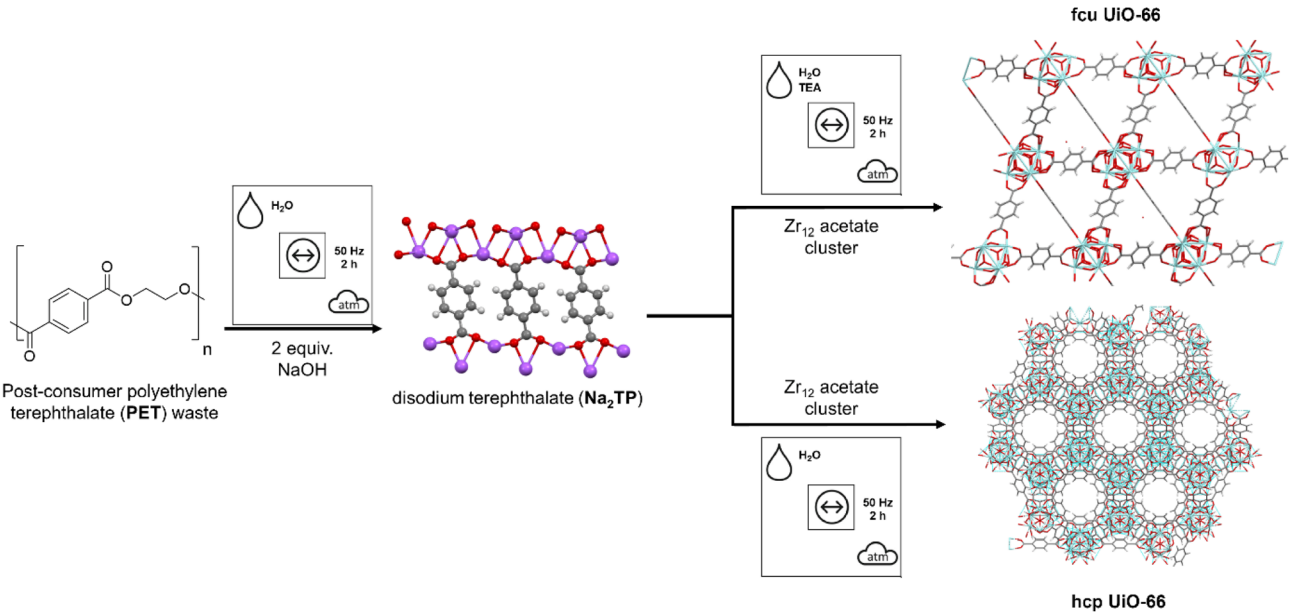

Fig. 1 Protocol for the selective mechanochemical conversion of post-consumer PET waste to fcu and hcp UiO-66 phases.

be achieved in as little as 20 min at 30 Hz using one 20 mm stainless steel ball in a 25 mL jar volume of the same material.[33] Similarly, a change in rheology to a gum-like or waxy mixture was found to be critical in achieving quantitative depolymerization. Based on gel permeation chromatography (GPC) analysis of molecular mass distribution, Tricker *et al.* postulated that individual polymer molecules are completely depolymerized in impact collisions, while others not involved in the collisions remain intact. Therefore, rapid depolymerization kinetics in the waxy phase, while the reaction mixture was coated on the milling ball, were attributed to an increasing number of individual impact collisions of PET polymer chains.

Also, mechanochemistry is known for the sustainable production of high-quality MOFs,[42] including conversion of terephthalate ligands from waste PET to value-added MOF materials.[43–46] Among them, UiO-66 is characterized by high chemical, thermal, and mechanical stability, and is the first reported zirconium-based MOF (fcu topology).[47] Its small-scale synthesis by ball milling has been reported.[48,49] Importantly, UiO-66 finds application in biomedicine,[50] catalysis,[51] and remediation of organic pollutants,[52] and is one of the handful of MOFs being produced on the commercial scale.[53–55] Besides the archetypal fcu UiO-66, a new hcp topology UiO-66 was first synthesized in 2018.[56] Recently, high-quality hcp phase UiO-66,[57] low-quality fcu phase UiO-66,[46] and a combination of both[58] were synthesized from chemically recycled terephthalate ligands coming from PET. In this work, we develop a protocol for the selective mechanochemical synthesis of high-quality UiO-66 fcu and hcp phases from PET post-consumer transparent bottles and coloured textile waste (Fig. 1).

Results and discussion

First, we tested the mechanochemical alkaline hydrolysis of PET using either sodium hydroxide (NaOH) or potassium hydroxide (KOH). Ball milling of PET with 2 equiv. of NaOH or KOH was performed in a 4 mL milling jar (more details in the SI) with one stainless steel milling ball (8 mm, 1.83 g) for 2 h. The analysis by powder X-ray diffraction (PXRD) showed that Na_2TP was obtained in the reaction with NaOH, but the sample contained a significant amount of amorphous content (Fig. 2a black). In the case of ball milling with KOH, PXRD analysis revealed the formation of dipotassium terephthalate (K_2TP), although not all diffraction peaks attributed to K_2TP were visible (Fig. 2b black). The apparent difference in reactivity between NaOH and KOH might result from differences in rheology. After milling with NaOH, the reaction mixture was in a compacted powder form spread homogeneously over the jar. On the other hand, the reaction mixture obtained by milling with KOH was a waxy substance, agglomerated around the milling ball and on both ends of the milling jar. Štrukil[32] and Tricker *et al.*[33] reported that coating on the milling and the formation of the waxy mixture when milling with NaOH was critical for the high PET depolymerization yields. In our case, the use of a smaller milling jar and ball might have prevented the necessary change in rheology when milling with NaOH.

Next, we turned to liquid-assisted grinding (LAG) conditions[59,60] using water as the liquid additive. Initial experiments with milling 150 mg of the reaction mixture (0.55 mmol of PET and 1.1 mmol of NaOH/KOH) using 30 μL of H_2O ($\eta = 0.2$) already showed an improvement in the crystallinity of the corresponding products (Fig. 2a and b red) and further increasing the η parameter resulted in higher-crystalline products (Fig. 2a and b blue). Therefore, all further experiments were conducted using LAG conditions with H_2O as the liquid additive. After optimization, we used TRIS synchrotron PXRD[61,62] to monitor the formation of crystalline Na_2TP and K_2TP during ball milling of PET with the corresponding hydroxides. In the case of milling PET with NaOH, the formation of crystalline Na_2TP could be observed after 8 min of the reaction (Fig. 3a). The crystallinity of

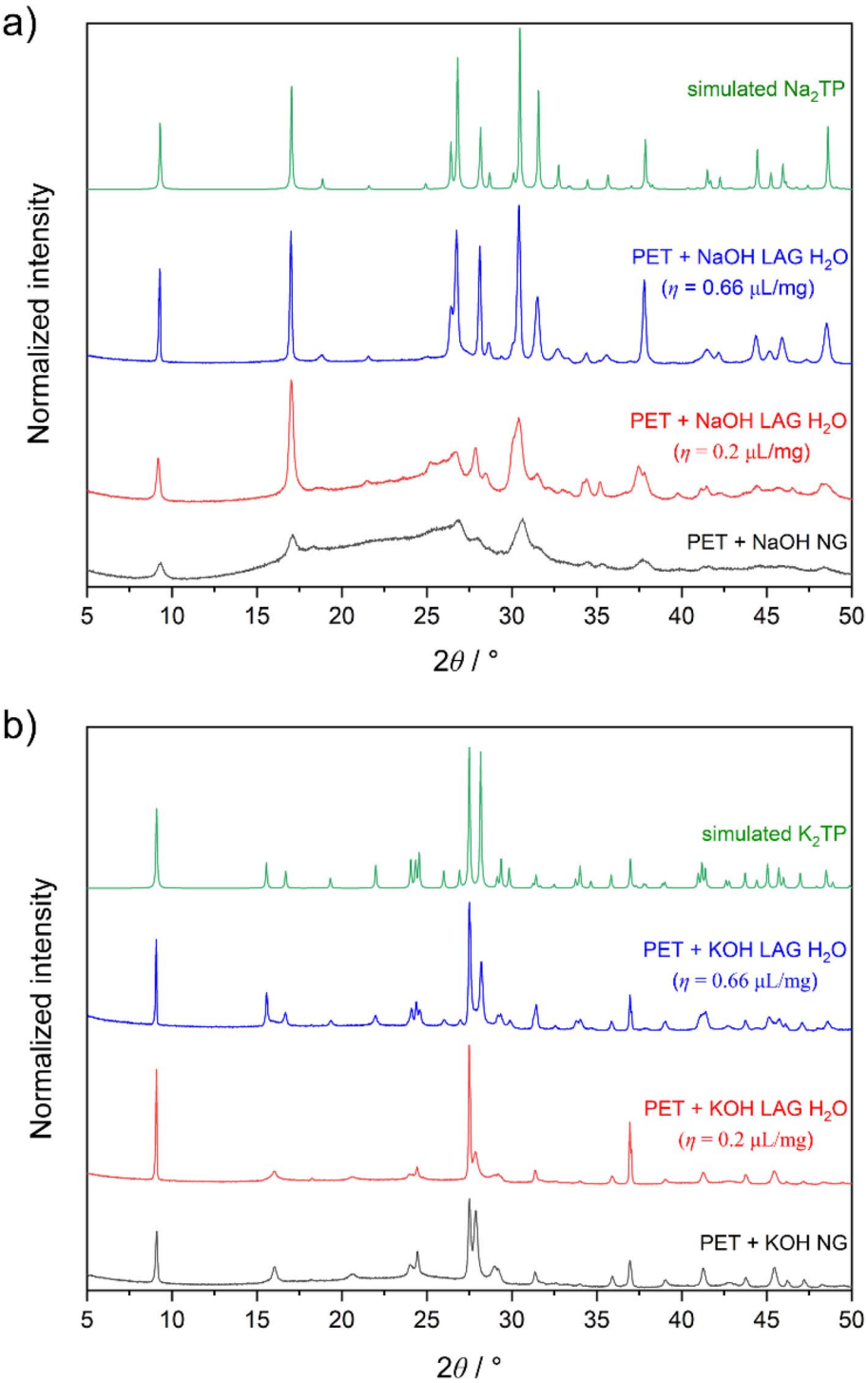

Fig. 2 PXRD patterns for milling PET under different conditions with (a) NaOH and (b) KOH (λ = 1.542 Å).

Na_2TP increased gradually until reaching a steady state after *ca.* 60 min of milling. Similarly, when milling PET with KOH using LAG conditions, the formation of crystalline K_2TP could be observed even faster, after 4 min of the reaction, and a steady state was reached after 20 min of milling (Fig. 3b). TRIS monitoring by Raman spectroscopy confirmed the faster kinetics for PET depolymerization when using KOH compared to NaOH. However, TRIS monitoring by Raman spectroscopy using the identical reaction conditions proved to be less sensitive, and the formation of K_2TP and Na_2TP was observed a bit later, specifically after 15 and 40 min, respectively (Fig. S1 and S2).

We then sought to correlate the formation of K_2TP and Na_2TP with the degree of PET depolymerization. We performed experiments on a 1 g scale using the same η parameter for 20,

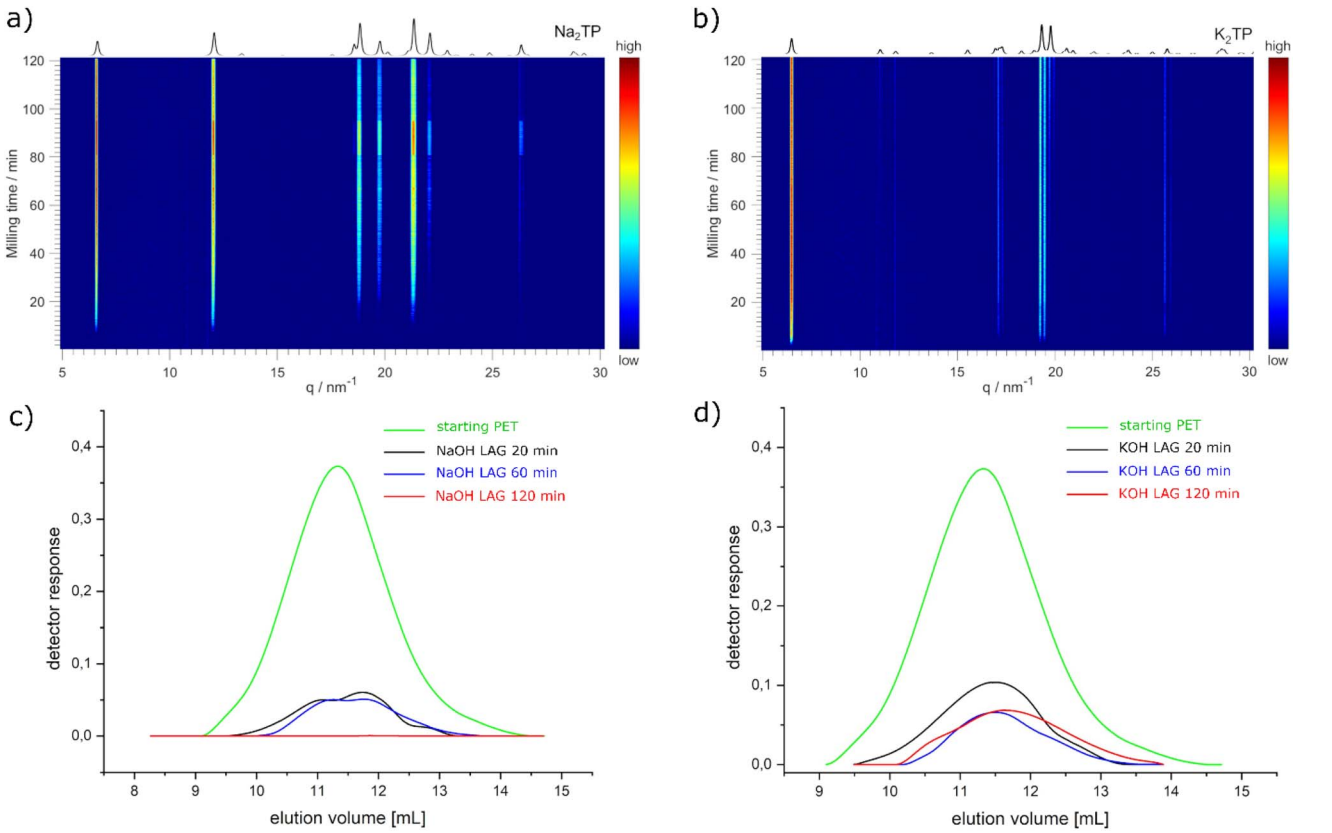

Fig. 3 TRIS synchrotron PXRD monitoring ($\lambda = 0.7295$ Å) of milling PET under LAG with H_2O: (a) with NaOH and (b) with KOH. GPC chromatograms for milling PET under LAG with H_2O: (c) with NaOH and (d) with KOH.

60, and 120 min and analysed them *ex situ* by PXRD and GPC. PXRD analysis demonstrated the gradual increase in the crystallinity of K_2TP and Na_2TP with increasing milling time (Fig. S3 and S4). We note minor differences compared to TRIS monitoring studies where steady states were observed faster. The latter might be due to the difference in the geometry and material composition of the milling jars when using lower reaction scales (for more details see SI). Nevertheless, GPC analysis for the reaction using NaOH correlated well with *ex situ* PXRD analysis and showed that the PET content decreases with increasing milling time (Fig. 3c) and after 120 min of milling, no PET was detected. The results of the reaction using KOH were a bit unexpected. After the initial decrease in PET content, no changes were detected when milling for 60 min and 120 min (Fig. 3d). This contrasts with PXRD analysis after milling PET with KOH for 120 min, which did not show a typical amorphous PET region in the diffractogram (Fig. S3). Interestingly, the difference in depolymerization of PET when using NaOH and KOH can be explained by rheology changes. In the former, a homogeneous wet paste was obtained after milling for 120 min (Fig. S5), whereas with KOH, a viscous gel was non-uniformly distributed in the jar under which solid powder was found (Fig. S6). To increase the depolymerization of PET using KOH, we carried out two new experiments, extending the milling time to three and four hours respectively. In both cases, however, we obtained a similar viscous gel under which traces of powder were found, and GPC analysis again showed the presence of approximately 9% PET (Fig. S7). We note here that under our LAG conditions using NaOH, coating on the ball was not observed as in the case of Štrukil[32] and Tricker *et al.*[33] but the rheology of the reaction mixture is important.[63] Based on GPC elution curves, largest polymer chains start to degrade first and after 60 min of milling with NaOH, there are no more chains longer than 10^5 g mol^{-1} (Fig. S8). As the depolymerization reaction by milling goes on, the number of polymer chains with 2×10^4 g mol^{-1} increases and the curve goes into bimodality, but there is no uniform shortening of the chains from polymers to oligomers and no signals are detected between 1500 and 100 g mol^{-1} (Fig. S8 and Table S1). Although the mechanochemical depolymerization of PET shows faster kinetics with KOH than with NaOH, unfavourable rheological changes hinder the complete depolymerization of PET with the former. Therefore, we decided to use NaOH as the base for the conversion of PET to UiO-66.

Firstly, we prepared $(Zr_6O_4(OH)4(CH_3COO)_{12})_2$ (zirconium acetate cluster) according to the previously published literature.[49] We chose to use a zirconium acetate cluster, instead of $ZrCl_4$ (ref. 46) or other zirconium sources,[48] due to its known use in benign mechanochemical synthesis of UiO-66 using H_2O as the liquid additive.[49] We then milled washed and dried Na_2TP (0.304 mmol, 63.9 mg), obtained after milling PET bottle with NaOH (Fig. S9 and S10), with zirconium acetate cluster

(0.0385 mmol, 131 mg), 85 μL of triethylamine (TEA, two equiv.), and 98 μL of H_2O. The reaction was performed in a 4 mL jar for 120 min at 50 Hz using one 8 mm SS ball (for more details see SI). We note that these conditions were adapted from the Karadeniz *et al.* who used a two-step protocol to first activate terephthalic acid by milling it with TEA and H_2O, after which a zirconium acetate cluster was added to the reaction mixture in the second milling step.[49] In our case, we attempted one-pot milling synthesis. The PXRD analysis confirmed the synthesis of high-crystallinity fcu UiO-66 phase (Fig. S11 magenta). When

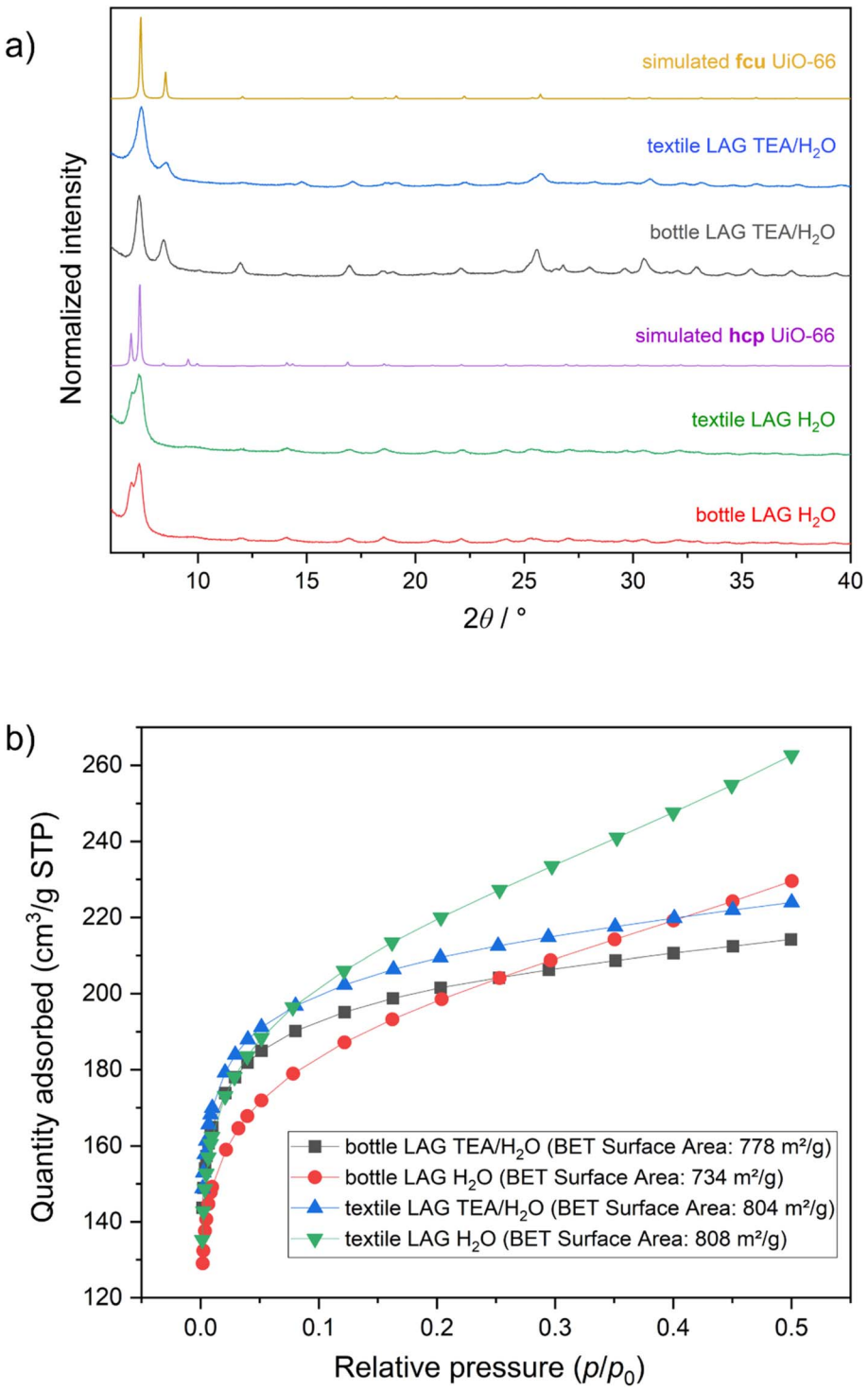

Fig. 4 (a) PXRD patterns for UiO-66 samples obtained in this work after the activation process and comparison to simulated patterns of fcu (CSD entry: RUBTAK03) and hcp (CSD entry: KINGUM) UiO-66 phases ($\lambda = 1.542$ Å). (b) Nitrogen adsorption isotherms measured at 77 K for UiO-66 samples shown in (a).

decreasing the volume of TEA to 42 μL (1 equiv.), an even higher crystallinity UiO-66 was obtained (Fig. S11 green). To see if UiO-66 can be accessed even without the use of a base, we milled Na_2TP (0.304 mmol, 63.9 mg), zirconium acetate cluster (0.0385 mmol, 131 mg), and 140 μL of H_2O. To our surprise, PXRD analysis showed that the crystalline product corresponded to UiO-66 hcp phase (Fig. 4a red). Furthermore, Fourier-transform infrared spectroscopy and thermogravimetric analysis showed similar spectra and thermal profile, respectively (Fig. S12–S16).

fcu-UiO-66 and hcp-UiO-66 are two distinct crystalline phases of UiO-66, which is composed of Zr(IV) metal clusters linked by benzene-1,4-dicarboxylate (BDC^{2-}, or terephthalate) ligands. The fcu phase represents the archetypal form of UiO-66 with a face-centred cubic topology, featuring $[Zr_6(\mu_3\text{-}O)_4(\mu_3\text{-}OH)_4(RCO_2)_{12}]$ hexanuclear secondary building units (SBUs, or clusters) that are 12-connected to the linkers, resulting in a Zr : BDC ratio of 1 : 1.[47] This structure includes triangular pore windows (~6 Å), tetrahedral pores (~8 Å), and octahedral cages (~11 Å). In contrast, the hcp phase adopts a hexagonal close-packed topology with larger $[Zr_{12}(\mu_3\text{-}O)_8(\mu_3\text{-}OH)_8(\mu_2\text{-}OH)_6(RCO_2)_{18}]$ dodecanuclear SBUs, formed by the condensation or merging of two hexanuclear clusters *via* bridging hydroxides.[56] These dodecanuclear clusters are 18-connected, leading to a ligand-deficient Zr : BDC ratio of approximately 1 : 0.75, and a pore structure with micropores around ~7 Å and ~10 Å. The hcp phase can be viewed as a condensed variant of the fcu phase, where synthetic conditions promote the aggregation of Zr_6 clusters into Zr_{12} double clusters, altering the overall packing and connectivity while maintaining the same chemical composition.

We then expanded our research to coloured post-consumer textile polyester (red sweater). This includes depolymerizing the initial red textile polyester to Na_2TP and developing decolorizing procedure using activated carbon (for details see SI, Fig. S17). We used de-colourized Na_2TP as a source of terephthalate ligands and performed LAG experiments (identical conditions to PET bottles) to access fcu and hcp UiO-66. In both cases, we obtained phase pure targeted UiO-66 phases (Fig. 4a blue and green, Fig. S12, S15 and S16). This confirmed that the selective mechanochemical access to fcu and hcp UiO-66 phases is independent of the starting PET waste source.

To validate the permanent porosity of mechanochemically synthesized UiO-66 materials, we performed nitrogen gas adsorption experiments (Fig. 4b and S18–S21). For that, selected UiO-66 samples were activated according to the previously published protocol.[48] All samples showed permanent porosity and exhibited gas adsorption isotherms typical for microporous samples (Fig. 4b). The quantity of adsorbed gas and the Brunauer–Emmett–Teller (BET) surface area is similar for all measured samples. For example, BET surface area of hcp UiO-66 from textile (808 $m^2\ g^{-1}$) and bottle PET (734 $m^2\ g^{-1}$) closely relates to the original report of hcp UiO-66 (874 $m^2\ g^{-1}$).[56] On the other hand, fcu UiO-66 samples obtained in this work (778 and 804 $m^2\ g^{-1}$) have slightly lower BET surface area compared to the previous report on mechanochemical synthesis of fcu UiO-66 using zirconium acetate cluster (1145 $m^2\ g^{-1}$).[49]

Conclusion

In conclusion, we have developed a protocol for the selective mechanochemical conversion of post-consumer PET bottles and textile waste into high-quality UiO-66 MOF materials, including the first ever synthesis of hcp UiO-66 by mechanochemistry. TRIS monitoring by synchrotron PXRD and Raman spectroscopy provided insights into the reaction dynamics and showed that, although hydrolysis with KOH initiates faster than with NaOH, it does not lead to complete PET depolymerization due to unfavourable rheological changes in the reaction mixture. Therefore, LAG conditions were shown to be a powerful tool to fine-tune mechanochemical PET depolymerization by alkaline hydrolysis. Based on our results, NaOH was used as the base for PET hydrolysis and further conversion to fcu and hcp UiO-66 phases. Interestingly, base-free mechanochemical route using water as a liquid additive leads to hcp UiO-66 phase, whereas adding a base results in fcu UiO-66 phase. Our results demonstrate that mechanochemistry is a powerful tool for converting post-consumer PET waste into phase-selective UiO-66 MOF materials.

Conflicts of interest

There are no conflicts to declare.

Data availability

The data supporting this article have been included as part of the supplementary information (SI). Supplementary information is available. See DOI: https://doi.org/10.1039/d4mr00126e.

Acknowledgements

T. S. is supported by the Add-on Fellowship of the Joachim Herz Foundation. We thank Ms. Tara Stolar for providing a red sweater as a source for polyester/PET. Beamtime at the BESSY II synchrotron (Helmholtz-Zentrum Berlin) on the μSPOT beamline is gratefully acknowledged for providing access to synchrotron X-ray diffraction facilities used in this work.

References

1 G. W. Coates and Y. D. Y. L. Getzler, *Nat. Rev. Mater.*, 2020, **5**, 501–516.
2 H. Li, H. A. Aguirre-Villegas, R. D. Allen, X. Bai, C. H. Benson, G. T. Beckham, S. L. Bradshaw, J. L. Brown, R. C. Brown, V. S. Cecon, J. B. Curley, G. W. Curtzwiler, S. Dong, S. Gaddameedi, J. E. García, I. Hermans, M. S. Kim, J. Ma, L. O. Mark, M. Mavrikakis, O. O. Olafasakin, T. A. Osswald, K. G. Papanikolaou, H. Radhakrishnan, M. A. Sanchez Castillo, K. L. Sánchez-Rivera, K. N. Tumu, R. C. Van Lehn, K. L. Vorst, M. M. Wright, J. Wu, V. M. Zavala, P. Zhou and G. W. Huber, *Green Chem.*, 2022, **24**, 8899–9002.

3 I. Vollmer, M. J. F. Jenks, M. C. P. Roelands, R. J. White, T. Van Harmelen, P. De Wild, G. P. Van Der Laan, F. Meirer, J. T. F. Keurentjes and B. M. Weckhuysen, *Angew. Chem., Int. Ed.*, 2020, **59**, 15402–15423.
4 J. Alić, M.-C. Schlegel, F. Emmerling and T. Stolar, *Angew. Chem., Int. Ed.*, 2024, e202414745.
5 J. Zhou, T. Hsu and J. Wang, *Angew. Chem., Int. Ed.*, 2023, **62**, e202300768.
6 S. Aydonat, A. H. Hergesell, C. L. Seitzinger, R. Lennarz, G. Chang, C. Sievers, J. Meisner, I. Vollmer and R. Göstl, *Polym. J.*, 2024, **56**, 249–268.
7 A. Briš, D. Margetić and V. Štrukil, *Green Chem.*, 2025, **27**, 14401–14435.
8 A. Rizzo and G. I. Peterson, *Prog. Polym. Sci.*, 2024, **159**, 101900.
9 J.-L. Do and T. Friščić, *ACS Cent. Sci.*, 2017, **3**, 13–19.
10 A. A. L. Michalchuk, E. V. Boldyreva, A. M. Belenguer, F. Emmerling and V. V. Boldyrev, *Front. Chem.*, 2021, **9**, 685789.
11 V. Martinez, T. Stolar, B. Karadeniz, I. Brekalo and K. Užarević, *Nat. Rev. Chem.*, 2022, **7**, 51–65.
12 K. J. Ardila-Fierro and J. G. Hernández, *ChemSusChem*, 2021, **14**, 2145–2162.
13 N. Fantozzi, J.-N. Volle, A. Porcheddu, D. Virieux, F. García and E. Colacino, *Chem. Soc. Rev.*, 2023, **52**, 6680–6714.
14 V. P. Balema, I. Z. Hlova, S. L. Carnahan, M. Seyedi, O. Dolotko, A. J. Rossini and I. Luzinov, *New J. Chem.*, 2021, **45**, 2935–2938.
15 Y. Chang, S. J. Blanton, R. Andraos, V. S. Nguyen, C. L. Liotta, F. J. Schork and C. Sievers, *ACS Sustain. Chem. Eng.*, 2024, **12**, 178–191.
16 G. Kim, B. Park, N. Kim, Y.-J. Hwang, A. Rizzo and G. I. Peterson, *Nat. Commun.*, 2025, **16**, 5924.
17 Y. Chang, A. H. Hergesell, C. L. Seitzinger, A. M. Hepstall, I. Vollmer and C. Sievers, *ACS Sustain. Chem. Eng.*, 2025, **13**, 18970–18982.
18 E. Jung, D. Yim, H. Kim, G. I. Peterson and T. Choi, *J. Polym. Sci.*, 2023, **61**, 553–560.
19 E. Jung, M. Cho, G. I. Peterson and T.-L. Choi, *Macromolecules*, 2024, **57**, 3131–3137.
20 V. S. Nguyen, Y. Chang, E. V. Phillips, J. A. DeWitt and C. Sievers, *ACS Sustain. Chem. Eng.*, 2023, **11**, 7617–7623.
21 L. Li, O. Vozniuk, Z. Cao, P. Losch, M. Felderhoff and F. Schüth, *Nat. Commun.*, 2023, **14**, 5257.
22 T. Morgen, S. Mecking and I. Vollmer, *Macromolecules*, 2025, **58**, 11388–11396.
23 L. Li, M. Leutzsch, P. Hesse, C. Wang, B. Wang and F. Schüth, *Angew. Chem., Int. Ed.*, 2025, **64**, e202413132.
24 K. Kubota, J. Jiang, R. Hisazumi, T. Endo, D. Miura, S. Kubo, S. Maeda and H. Ito, *J. Am. Chem. Soc.*, 2024, **146**, 1062–1070.
25 A. H. Hergesell, R. J. Baarslag, C. L. Seitzinger, R. Meena, P. Schara, Ž. Tomović, G. Li, B. M. Weckhuysen and I. Vollmer, *J. Am. Chem. Soc.*, 2024, **146**, 26139–26147.
26 A. H. Hergesell, C. L. Seitzinger, H. Pasternak, L. Seidling, V. M. Ospina Guarin, N. Karpensky, F. Puch, T. Welzel and I. Vollmer, *Catal. Sci. Technol.*, 2025, **15**, 7525–7538.
27 A. H. Hergesell, C. L. Seitzinger, J. Burg, R. J. Baarslag and I. Vollmer, *RSC Mechanochem.*, 2025, **2**, 263–272.
28 M. Pérez-Venegas, T. Friščić and K. Auclair, *ACS Sustain. Chem. Eng.*, 2023, **11**, 9924–9931.
29 A. S. Makarov and M. Rueping, *Green Chem.*, 2025, **27**, 716–721.
30 D. Jain, F. Cramer, P. Shamraienko, H.-J. Drexler, B. Voit and T. Beweries, *RSC Sustainability*, 2025, **3**, 3513–3519.
31 K. Kubota, R. Hisazumi, K. Jana, J. Jiang, T. Endo, S. Maeda and H. Ito, *J. Am. Chem. Soc.*, 2026, DOI: 10.1021/jacs.5c20376.
32 V. Štrukil, *ChemSusChem*, 2021, **14**, 330–338.
33 A. W. Tricker, A. A. Osibo, Y. Chang, J. X. Kang, A. Ganesan, E. Anglou, F. Boukouvala, S. Nair, C. W. Jones and C. Sievers, *ACS Sustain. Chem. Eng.*, 2022, **10**, 11338–11347.
34 S. Kaabel, J. P. D. Therien, C. E. Deschênes, D. Duncan, T. Friščić and K. Auclair, *Proc. Natl. Acad. Sci. U. S. A.*, 2021, **118**, e2026452118.
35 H. W. Lee, K. Yoo, L. Borchardt and J. G. Kim, *Green Chem.*, 2024, **26**, 2087–2093.
36 E. Anglou, A. Ganesan, Y. Chang, K. M. Gołąbek, Q. Fu, W. Bradley, C. W. Jones, C. Sievers, S. Nair and F. Boukouvala, *Chem. Eng. J.*, 2024, **481**, 148278.
37 E. Anglou, Y. Chang, W. Bradley, C. Sievers and F. Boukouvala, *ACS Sustain. Chem. Eng.*, 2024, **12**, 9003–9017.
38 S. Chrea and A. Takagaki, *Chem. Commun.*, 2025, **61**, 7474–7477.
39 P. M. Rincon, M. Renner, L. Borchardt and P. Biessey, *Chem. Eng. J.*, 2025, **509**, 161411.
40 E. Anglou, F. Boukouvala and P. M. Stathatou, *Chem. Eng. J.*, 2025, 168719.
41 K. Gołąbek, Y. Chang, L. R. Mellinger, M. V. Rodrigues, C. De Souza Coutinho Nogueira, F. B. Passos, Y. Xing, A. Ribeiro Passos, M. H. Saffarini, A. B. Isner, D. S. Sholl and C. Sievers, *Chem*, 2025, 102754.
42 T. Stolar and K. Užarević, *CrystEngComm*, 2020, **22**, 4511–4525.
43 T. S. Crickmore, H. B. Sana, H. Mitchell, M. Clark and D. Bradshaw, *Chem. Commun.*, 2021, **57**, 10592–10595.
44 Y. She, W. Han, H. Liu, G. Hu, H. Wang, X. Wen, L. Liu, L. Feng, X. Zhang and J. Gong, *Chem. Eng. J.*, 2025, **515**, 163895.
45 Z. Gong, Z.-K. Dai, Z.-Y. Dong, Q.-X. Liu, V. A. Milichko, H.-J. Liu, J. Liu, R. Niu and J. Gong, *Rare Met.*, 2024, **43**, 3833–3843.
46 P. He, Z. Hu, Z. Dai, H. Bai, Z. Fan, R. Niu, J. Gong, Q. Zhao and T. Tang, *ChemSusChem*, 2023, **16**, e202201935.
47 J. H. Cavka, S. Jakobsen, U. Olsbye, N. Guillou, C. Lamberti, S. Bordiga and K. P. Lillerud, *J. Am. Chem. Soc.*, 2008, **130**, 13850–13851.
48 K. Užarević, T. C. Wang, S.-Y. Moon, A. M. Fidelli, J. T. Hupp, O. K. Farha and T. Friščić, *Chem. Commun.*, 2016, **52**, 2133–2136.
49 B. Karadeniz, A. J. Howarth, T. Stolar, T. Islamoglu, I. Dejanović, M. Tireli, M. C. Wasson, S.-Y. Moon, O. K. Farha, T. Friščić and K. Užarević, *ACS Sustain. Chem. Eng.*, 2018, **6**, 15841–15849.

50 I. Abánades Lázaro and R. S. Forgan, *Coord. Chem. Rev.*, 2019, **380**, 230–259.
51 M. Rimoldi, A. J. Howarth, M. R. DeStefano, L. Lin, S. Goswami, P. Li, J. T. Hupp and O. K. Farha, *ACS Catal.*, 2017, **7**, 997–1014.
52 C. A. Clark, K. N. Heck, C. D. Powell and M. S. Wong, *ACS Sustain. Chem. Eng.*, 2019, **7**, 6619–6628.
53 Zirconium (CAS Number 1072413-89-8) : Strem Product Catalog, https://www.strem.com/en-DE/product/zirconium-14dicarboxybenzene-mof-uio66/01tVN000003kBuxYAE, accessed 15 May 2024.
54 Products | ProfMOF - Metal Organic Frameworks, https://profmof.com/products/, accessed 15 May 2024.
55 UiO-66, https://novomof.com/technology/uio-66/, accessed 15 May 2024.
56 M. Ermer, J. Mehler, M. Kriesten, Y. S. Avadhut, P. S. Schulz and M. Hartmann, *Dalton Trans.*, 2018, **47**, 14426–14430.
57 L. Zhou, S. Wang, Y. Chen and C. Serre, *Microporous Mesoporous Mater.*, 2019, **290**, 109674.
58 P. Agola and M. Taddei, *RSC Sustainability*, 2026, DOI: 10.1039/D5SU00463B.
59 N. Shan, F. Toda and W. Jones, *Chem. Commun.*, 2002, 2372–2373.
60 T. Friščić, A. V. Trask, W. Jones and W. D. S. Motherwell, *Angew. Chem., Int. Ed.*, 2006, **45**, 7546–7550.
61 A. A. L. Michalchuk and F. Emmerling, *Angew. Chem., Int. Ed.*, 2022, **61**, e202117270.
62 S. Lukin, L. S. Germann, T. Friščić and I. Halasz, *Acc. Chem. Res.*, 2022, **55**, 1262–1277.
63 B. P. Hutchings, D. E. Crawford, L. Gao, P. Hu and S. L. James, *Angew. Chem., Int. Ed.*, 2017, **56**, 15252–15256.